GKSS
FORSCHUNGSZENTRUM
in der HELMHOLTZ-GEMEINSCHAFT

Final Draft
of the original manuscript:

Clemens, H.; Chladil, H.F.; Wallgram, W.; Zickler, G.A.; Gerling, R.;
Liss, K.-D.; Kremmer, S.; Guether, V.; Smarsly, W.:

In and ex situ investigations of the Beta-phase in a Nb and Mo containing Gamma-TiAl based alloy

In: Intermetallics (2008) Elsevier

DOI: 10.1016/j.intermet.2008.03.008

Manuscript

In- and ex-situ investigation of the β-phase in a Nb and Mo containing γ-TiAl based alloy

H. Clemens[a,*], H. F. Chladil[a], W. Wallgram[a], G. A. Zickler[b], R. Gerling[c], K.-D. Liss[d], S. Kremmer[e], V. Güther[f], W. Smarsly[g]

[a] Department of Physical Metallurgy and Materials Testing, Montanuniversität, A-8700 Leoben, Austria

[b] Christian Doppler Laboratory for Early Stages of Precipitation, A-8700 Leoben, Austria

[c] Institute of Materials Research, GKSS Research Centre, D-21502 Geesthacht, Germany

[d] Bragg Institute, Australian Nuclear Science and Technology Organisation, Lucas Heights NSW 2234, Australia

[e] Böhler Schmiedetechnik GmbH&Co KG, A-8605 Kapfenberg, Austria

[f] GfE Metalle und Materialien GmbH, D-90431 Nuremberg, Germany

[g] MTU Aero Engines GmbH, D-80995 Munich, Germany

* Corresponding author. Tel.: ++43 3842 402 4200; fax: ++43 3842 402 4202.

E-mail address: helmut.clemens@unileoben.ac.at (H. Clemens).

Dedicated to Dr. Arno Bartels on the occasion of his 65th birthday

Abstract

In a β-stabilised Ti-43Al-4Nb-1Mo-0.1B alloy (composition in atomic percent) the correlation between the occurrence of β-phase and temperature was analyzed experimentally and compared to thermodynamic calculations. Results from in-situ high-energy X-ray diffraction,

texture measurements, heat-treatments, scanning electron microscopy, and temperature-dependent flow stress measurements were used to study the evolution of the β-phase with temperature. Thermodynamic calculations based on the CALPHAD method were applied to correlate the phases developed in the β-solidifying TiAl based alloy under investigation. This alloy is characterized by an adjustable β-phase volume fraction at temperatures where hot-work processes such as forging and rolling are conducted. Due to a high volume fraction of β-phase at elevated temperatures the hot-extruded alloy can be forged under near conventional conditions.

Key words: A. titanium aluminides, based on TiAl; B. alloy development; C. phase transformation, phase prediction; D. deformation behaviour, conventional forging.

1. Introduction

The continuous demand for weight reduction and higher engine efficiencies in automotive, aerospace and energy industries pushes the materials applied today towards their limits. Therefore, these industries have a strong need for developing novel light-weight materials which can withstand temperatures up to 800°C, while maintaining acceptable mechanical properties. Intermetallic γ-TiAl based alloys are certainly among the most promising candidates to fulfill the required thermal and mechanical specifications [1-3]. Especially, TiAl alloys with high Nb-contents, showing a baseline composition of Ti-(42-45)Al-(5-10)Nb (at.%), have attracted much attention because of their high creep strength, good ductility at room temperature and excellent oxidation resistance [1-6]. Nb reduces the stacking fault energy in γ-TiAl, retards diffusion processes and modifies the structure of the oxidation layer

[2,4,6]. Cast alloys based on Ti-45Al, which solidify via the β-phase, exhibit an isotropic, equiaxed and texture-free microstructure with modest micro-segregation, whereas peritectic alloys (solidification via the α-phase) show anisotropic microstructures as well as significant texture and segregation [7,8]. Alloy design concepts for γ-TiAl based alloys showing refined cast microstructures were recently reported by Imayev et al. [9]. In order to increase the economic feasibility of wrought processing for the manufacture of γ-TiAl components, alloys are needed which can be processed "near conventionally", e.g. a conventional forging equipment with minor and inexpensive modifications can be used. Thus, a fine-grained casting microstructure is favourable to both, ingot breakdown and secondary forming operations [2,3]. The alloys should be designed to allow for robust industrial heat-treatments, i.e. the alloy must tolerate a specified (and realistic) variation of the constituting elements, without pronounced changes of phase transition temperatures and phase volume fractions and related variations in mechanical properties. An alloy design strategy to improve the hot-workability of TiAl alloys is to exploit a combination of thermo-mechanical processing and additional alloying elements to induce the disordered β-phase at elevated temperatures as ductile phase [10-13]. The disordered β-phase with bcc lattice provides a sufficient number of independent slip systems. Thus, it may improve the deformability at elevated temperature, where, for example, processes such as rolling and forging are performed. Several authors [10,13-19] have demonstrated that, by stabilizing the β-phase through alloying with Nb, Ta, Mo or other elements, an improvement in hot-workability can be achieved and novel types of microstructures can be adjusted by exploiting a multitude of solid-state transformations. From a processing related point of view the alloy should fulfil the following demands: (i) after casting and solidification, the alloy should possess a refined equiaxed microstructure with no significant casting texture. (ii) The composition of the alloy must be defined to ensure a solidification path according to $L \rightarrow L + \beta \rightarrow \beta \rightarrow \ldots$, instead of a peritectic solidification pathway, $L \rightarrow L + \beta \rightarrow \alpha \rightarrow \ldots$, which is prone to segregation [7,9]. (iii) During ingot

breakdown as well as secondary hot-forming operations a significant volume fraction of disordered β-phase should be present, which improves the deformability at elevated temperature and suppresses grain growth. At service temperature, however, the volume fraction of the β-phase, which then shows an ordered B2 structure, should be insignificant in order not to deteriorate creep properties [20]. (Note: in the following B2 is referred to as β/B2 unless stated otherwise). (iv) In order to avoid uncontrollable grain coarsening effects during hot-processing as well as during adjustment of the microstructure through subsequent heat-treatments the existence of a single phase region at elevated temperatures should be avoided, i.e. transitions such as $\alpha + \gamma \rightarrow \alpha$ must be suppressed. Another possibility is to keep the α-phase region very small. In this case the single α-field can be passed without significant grain coarsening as long as the dissolution kinetics of the β/B2-phase is decelerated by the presence of alloying elements with a low diffusibility, e.g. Nb and Mo.

2. Alloy selection and experimental

In order to select an alloy which fulfills the demands as defined in the previous section, thermodynamic calculations based on the CALPHAD method were conducted for the prediction of the constituent phases and the related transition temperatures. Two different software packages - ThermoCalc® and MatCalc - were applied using the same commercial TiAl database [21]. In recent publications, however, the thermodynamic database used was found to poorly describe the transition temperatures and phase proportions in high Nb bearing γ-TiAl based alloys as reported in [15,22]. Therefore, it should be pointed out that the following calculation was conducted to study alloying trends rather than to give absolute values on phase fractions and transition temperatures. Figure 1 shows the calculated phase fractions as a function of temperature for the investigated Ti-43Al-4Nb-1Mo-0.1B alloy. Nb

decreases the stacking fault energy in γ-TiAl, slows down diffusion processes in both, γ-TiAl and α_2-Ti_3Al and improves the oxidation behaviour [2,4,6]. Like Nb, Mo raises the activation energy of diffusion in γ and α_2, but exhibits a much higher partition coefficient $k_{\beta\alpha}$ than Nb [23]. It must be taken into account that phases, when stabilized by such slow-diffusing elements, are expected to exhibit a sluggish dissolution behaviour. A boron content of 0.1 at% was selected to ensure a grain refining effect during solidification [24,25]. Boron, which tends to form very stable borides is also beneficial in case of heat-treatments conducted at high temperatures. Here, the borides retard grain coarsening by pinning of the grain boundaries [3,25]. In addition, the borides favour the formation of the lamellar microstructure ($\alpha \rightarrow \alpha + \gamma$) over the massive transformation ($\alpha \rightarrow \gamma_M$) by heterogeneous nucleation of γ-lamellae [24,25]. From Figure 1 it is evident that Ti-43Al-4Nb-1Mo-0.1B solidifies entirely via the β-phase. Furthermore, the mole fraction of the β-phase shows a minimum around 1250°C. It should be noted that below the temperature of the minimum the mole fraction of the β-phase slightly increases or shows an approximately unchanging value. Below the eutectoid temperature (~ 1115°C) the β-phase fraction decreases with decreasing temperature and seems to vanish at about 600°C. From the phase predictions shown in Figure 1 it is obvious that the chosen alloy exhibits no single phase region at temperatures below 1400°C. However, it must be kept in mind that Figure 1 predicts phase conditions present under thermodynamic equilibrium and that the used database has already shown an inaccuracy in the prediction of phase proportions in γ-TiAl based alloys possessing high Nb concentrations [15,22]. However, γ-TiAl based alloys, when processed under technical relevant conditions, always show a more or less pronounced deviation from phase equilibrium which makes any comparison difficult.

Ti-43Al-4Nb-1Mo-0.1B ingots with 65 mm (experimental ingots) and with 230 mm (large-scale ingots) in diameter were prepared by GfE Metalle und Materialien GmbH, Nuremberg, Germany, by means of double vacuum arc melting using commercially pure charge materials

and master alloys. The total amount of interstitial impurities was well below 750 mass-ppm. For details concerning ingot processing the reader is referred to reference [26]. The large-scale ingot was protected with a diffusion barrier, canned in steel and hot-extruded below T_α to a diameter of about 50 mm of TiAl core material. After extrusion a stress-relieve heat-treatment was applied (950°C/4hrs/furnace cooling).

The distribution and constitution of the phases in the as-cast as well as hot-extruded and stress-relieved alloy was analyzed using a Zeiss Evo 50 scanning electron microscope (SEM) equipped with an Oxford Instruments Inco Crystal 300.

For texture analysis of the as-cast alloy neutron diffraction was applied which allows examination of the whole body of a sample of some cubic centimetres [7]. The measurements were carried out at the TEX-2 diffractometer of GKSS Research Centre using cylindrical specimens of 10 mm in diameter, which were cut from the centre of an experimental Ti-43Al-4Nb-1Mo-0.1B ingot, parallel to its symmetry axis. Quantitative textures were calculated using the iterative series expansion method proposed by Dahms and Bunge [27] with a degree of series expansion of lmax = 22. The advantage of this method is that fewer pole figures are required when compared with standard series expansion methods.

In-situ high-energy X-ray diffraction (HE-XRD) studies regarding the occurring solid-state phase transformations and the temperature dependence of the β-phase were performed at the beamline ID15B at the European Synchrotron Radiation Facility (ESRF) in Grenoble, France. For the experiment, a custom-made diffraction furnace was used which heated the specimen up to 1400°C. Heating was conducted under constant flow of helium to avoid oxidation of the sample surface. The furnace had an entrance hole for the primary X-ray beam and an exit window for the scattering intensity (Debye-Scherrer rings) with an opening angle of 15°. Both X-ray windows were equipped with foils of polyimide (Kapton®, DuPont®, Wilmington, DE, USA) in order to hold the controlled atmosphere. The samples were machined to geometries of cylinders with a diameter of 4 mm and were mounted on a ceramic sample holder for the

in-situ diffraction furnace. The specimen were continuously heated to 800°C with a heating rate of 5 K min^{-1} and further heated to 1400°C with 2 K min^{-1}. Monochromatic synchrotron radiation with a nominal energy of 89.05 keV and an energy resolution of $\Delta E/E = 10^{-3}$ was used. The cross-section of the primary beam at the sample position was defined as 100 × 100 μm^2. The intensity of the primary beam was measured by a photo diode. HE-XRD patterns were taken continuously during the in-situ heat treatment with a time interval of 2 min between two measurements. The specimen was continuously rotated during exposure to avoid texture effects and obtain smooth Debye-Scherrer rings. A two-dimensional image plate detector (mar345, Marresearch, Norderstedt, Germany) with a resolution of 2300 × 2300 pixels (pixel size: 150 × 150 μm^2) was used for detecting the scattered photons. The diffraction patterns covered a range of scattering vector of 2.8 $nm^{-1} < q < 64$ nm^{-1}, where the length of the scattering vector is given by $|\mathbf{q}| = q = (4\pi / \lambda) \sin \theta$, with 2θ being the scattering angle and λ the wavelength. An exposure time of 20 s yielded a diffraction pattern with excellent counting statistics. The average readout of the detector data took 90 s. The diffraction patterns were corrected for background scattering and were normalized to the primary intensity of the synchrotron X-ray flux by using the data reduction software program FIT2D [28]. The measurements showed isotropic Debye-Scherrer diffraction rings, which were azimuthally averaged for equal radial distances from the central X-ray beam.

In order to study the deformation (plastic flow) behaviour of alloy Ti-43Al-4Nb-1Mo-0.1B, cylindrical specimens with dimension Ø 4mm x 10mm were cut from stress-relieved hot-extruded material. The experiments were performed in a deformation dilatometer DIL805A/D supplied by Bähr-Thermoanalyse GmbH. The samples were heated under helium atmosphere up to temperatures in the range of 1240 to 1300°C, held for 10 min and then deformed at rates between 0.05 to 0.5 s^{-1}.

Forging tests on an industrial scale were performed on a conventional 10 MN hydraulic press without any special isothermal forging equipment. However, due to the high strain rate

sensitivity of γ-TiAl alloys and thus the low die speed in the forging process, the dies were pre-heated prior to forging to avoid excessive cooling during deformation. The die temperature during forging was approximately 400 - 800°C below the billet temperature. The hydraulic press has been specially automated for low die speeds and to allow an exact control of die speed, position and temperature during the whole process. The billets for the forging experiments on an industrial scale were produced via the ingot metallurgy route as described above. After extrusion the material is cut into cylinders between 40 and 80 mm in length and mechanically turned to a diameter of 40 or 50 mm. Prior to forging a heat shielding layer is applied to the billet to reduce heat loss during transfer from the furnace to the press as well as during the initial forging process. The billet was heated up to a forging temperature above T_α in an electric furnace under argon atmosphere [18]. After holding on temperature for a defined time the billet was manually transferred into the press within 5sec and the forging process is started. The total contact time between the billet and the dies can last up to 60 sec depending on die speed and total stroke. More information on the industrial forging process is given by Kremmer et al. [18].

3. Results and discussions

Figure 2a shows the microstructure of alloy Ti-43Al-4Nb-1Mo-0.1B in as-cast condition. The microstructure can be explained by a complete solidification via the β-phase [7,9,17] as predicted in Figure 1. It consists of equiaxed lamellar ($\gamma + \alpha_2$)-colonies with a colony diameter of about 100 µm. The β/B2-phase is mainly located along colony boundaries and only a small volume fraction is present within the colonies. In addition, the existence of rod- shaped Ti-borides, enriched in Nb and Mo, was detected [16,17]. EDX analysis has provided evidence that the β-phase is more enriched in Mo than in Nb, which confirms that Mo exhibits a higher

partition coefficient $k_{\beta\alpha}$ than Nb [23]. From this observation it is assumed that both β-stabilizing elements have segregated to β/α-interface boundaries in the course of the $\beta \rightarrow \alpha$ transformation. However, the β/B2-phase does not form a complete layer around the lamellar colonies, but is intersected by small γ-grains. According to Zhang et al. [24] the mixture of β/B2 and γ grains as shown in the inset of Figure 2a results from the cellular (discontinuous) reaction $\beta \rightarrow \beta + \gamma$. At room temperature the as-cast material shows a high amount of β/B2-phase which is inconsistent with the thermodynamic calculation shown in Figure 1. This behaviour might be attributed to both, the high solidification and cooling rates. This finding also implies that a considerable amount of β/B2 must exist in a metastable state. For the sake of completeness it should be mentioned that the as-cast microstructure (Figure 2a) can further be refined by subsequent heat-treatments. Annealing in the temperature range of 1250 - 1400°C followed by air cooling leads to colony sizes well below 50 μm as reported by H. Chladil et al. [17]. Recently, for a comparable alloy system similar results have been reported by Imayev et al. [9].

Figure 2b shows alloy Ti-43Al-4Nb-1Mo-0.1B after hot-extrusion below the α-transus temperature ($T_\alpha \sim 1260$°C, as determined by DSC measurements [16]). During extrusion a refinement of the ingot microstructure took place and the β/B2-phase has been aligned in extrusion direction which also was observed for the borides [16]. After extrusion a stress-relieve heat-treatment at 950°C was applied [17].

Figure 3 shows the 110 pole figure of the γ-TiAl phase present in the cast Ti-43Al-4Nb-1Mo-0.1B ingot. With a maximum pole density of 1.8 multiple random distribution, no statistically significant texture is prevailing after solidification via $L \rightarrow L + \beta \rightarrow \beta$ and the subsequent phase transformations which occur during cooling to room temperature. In contrast, the insert in Figure 3 displays the 110 pole figure of a Ti-48Al alloy after peritectic solidification [7]. Here, a pronounced preferential orientation of the γ-grains is evident. As the pole figure

shows that a preferential alignment of <110] directions perpendicular to the symmetry axis occurred. This texture corresponds to that usually observed for cast γ-TiAl alloys [29,30] and can be explained by a [0001] dendrite orientation of the hexagonal α-phase with respect to the heat flow direction. In conclusion, the microstructural observation of equiaxed solidification of the β-stabilized Ti-43Al-4Nb-1Mo-0.1B alloy agrees with the results of texture analysis. The absence of a casting texture is beneficial as far as subsequent hot-forming operations are concerned.

Figure 4 shows four azimuthally averaged HE-XRD patterns (Debye-Scherrer rings) of the alloy Ti-43Al-4Nb-1Mo-0.1B for 21°C (Figure 4a), 1179°C (Figure 4b), 1259°C (Figure 4c), and 1320°C (Figure 4d). In the initial state (Figure 4a) the diffraction pattern solely contains peaks from the phases α_2-Ti_3Al, γ-TiAl and β/B2-Ti. The diffraction peaks of α_2-002 and γ-111 are completely overlapping and appear as one single peak at q = 27.20 nm^{-1}. The diffraction peaks of γ-002 and γ-200 at q = 31.15 nm^{-1} and q = 31.55 nm^{-1}, respectively, are clearly separated due to slight differences in the lattice spacing along the a and c axis of the tetragonal γ-TiAl crystal unit cell ($L1_0$ structure). With increasing temperature, the diffraction peaks are shifted towards lower q values because of thermal expansion of the crystal lattice. The transformation $\alpha_2 \rightarrow \alpha$ takes place at the eutectoid temperature, which is indicated by the appearance of the disordered α-Ti phase. The order-disorder transition is accompanied by a reduction of the size of crystal unit cell with the reciprocal lattice correlation α_2-200 ≡ α-100 at $q \approx 25.2$ nm^{-1} and α_2-002 ≡ α-002 at $q \approx 27.0$ nm^{-1}. Therefore, the superstructure diffraction peak α_2-101 at q = 18.6 nm^{-1} disappears. The eutectoid temperature was determined to be about 1165°C, which matches well with the result obtained from differential scanning calorimetry (DSC) measurements [16,17], but is about 50°C above that predicted by the phase fraction calculations (Figure 1). Figure 4b illustrates the diffraction pattern in the phase field α + β/B2 + γ at 1179°C above the eutectoid temperature.

The thermodynamic equilibrium calculations shown in Figure 1 indicate a minimum of the β/B2-phase fraction at about 1260°C, which is confirmed by the diffraction pattern at 1259°C (Figure 4c), where the intensities of the B2-100 and B2-110 diffraction peaks at q = 19.20 nm^{-1} and q = 27.35 nm^{-1}, respectively, show a minimum. As visible in Figure 4d, the diffraction pattern significantly changes at temperatures above α-transus, where the phase γ-TiAl disappears and the alloy only contains β/B2-phase and α-phase. Figure 4d shows the presence of α, β and B2 phases above the α-transus temperature, which indicates that disordered β and ordered B2 coexist up to high temperatures, presumably forming a domain structure. This finding is in agreement with thermodynamic calculations (Figure 1), where the presence of B2 is predicted up to about 1410°C. However, the β/B2 coexistence is in partial contradiction with the demand of a disordered bcc high-temperature phase (see Introduction). Nevertheless, one can speculate about the difference in the deformation behaviour of β and B2 at such high temperatures. This question, however, will be topic of further studies. The HE-XRD measurements provide no evidence for passing through a single α phase field, which is in agreement with the thermodynamic equilibrium calculation (Figure 1). However, previous studies have shown that the thermodynamic databank used was found to poorly describe the transition temperatures and phase proportions in high-alloyed γ-TiAl based alloys [15,16,22]. In addition, the heating rate of 2 K min^{-1} might be too fast for reaching the thermodynamic equilibrium if the single α phase field is rather small and/or the β/B2-phase shows a slow dissolution kinetic. In the temperature range above α-transus, the two-dimensional diffraction patterns (area detector images) indicate a evolution from sharp and well defined Debye-Scherrer rings to more or less regular diffraction spots relating to local reciprocal lattice maps from a few single crystallites (see reference [31]). This effect is due to significant grain growth above the α-transus temperature and the remaining low number of

illuminated crystallites. Table 1 summarizes the transformation temperatures of the alloy Ti-43Al-4Nb-1Mo-0.1B determined by in-situ HE-XRD.

In order to check the appearance of the minimum of the β/B2-phase as predicted by phase calculations (Figure 1), an annealing treatment has been conducted. Figure 5 shows the microstructure of a sample with an actual Al content of 43.8 at% which was annealed at 1270°C for 3 hrs followed by air cooling. The microstructure of the starting material is depicted in Figure 2b. From Figure 5 it is evident that during annealing the α-grains have grown and the β/B2-phase almost disappeared. However, a small volume fraction of β/B2-phase was still present (along with the borides) preventing catastrophic grain growth. Many of the β-particles are situated along former α-grain boundaries and triple points contributing to the so-called "Zener-drag" mechanism [33]. Again, the question if the predicted minimum of the β/B2-phase is real or if a small single α-phase field still exists can not be answered unambiguously. Although a holding time of 3 hrs was used in this experiment the existence of a single α-phase field can be masked if the (metastable) β/B2-phase exhibits a rather slow dissolution behaviour. In order to answer this question further experiments are in progress and the results will be reported in a forthcoming paper.

Figure 6 depicts schematically the dependence of the flow stress on temperature and strain rate. The flow stress shows a distinct strain rate dependency, which is a specific behaviour of γ-TiAl based alloys [34]. Of particular interest, however, is the pronounced flow stress peak. The temperature of the peak maximum corresponds with that temperature where CALPHAD predicts the minimum fraction of β/B2-phase (Figure 1). For a deformation temperature below the peak maximum the flow stress decreases as it decreases for temperatures above the flow stress maximum. The behaviour of the flow stress correlates directly with the volume fractions of the β/B2-phase at the respective temperatures. Therefore, it is tempting to speculate that the β/B2-phase with bcc lattice provides a sufficient number of independent slip

systems. Thus, it improves the deformability at elevated temperature, where, for example, processes such as rolling and forging are carried out.

The hot-workability of alloy Ti-43Al-4Nb-1Mo-0.1B was evaluated by performing various forging experiments using a parameter matrix of different billet dimensions, billet temperatures, die temperatures, and die speeds. In Figure 7a a representative result of a forging experiment is shown. The pancake was forged to an overall strain of 1.3. The microstructure after forging is displayed in Figure 7b. At room temperature the microstructure consists of lamellar (α_2 + γ)-colonies with β-phase situated on colony boundaries and triple points. Analysing all forging experiments, it was found that the forging window of alloy Ti-43Al-4Nb-1Mo-0.1B is significantly extended when compared to other high Nb bearing γ-TiAl based alloys [18]. The observed widening can mainly be attributed to the presence of the bcc β-phase at forging temperature and its influence on the deformation behaviour (Figure 6). Finally, Figure 7c shows a blade pre-form made of alloy Ti-43Al-4Nb-1Mo-0.1B. More information on the blade forging process is reported in refs. [18].

4. Summary

Thermodynamic calculations based on the CALPHAD method were used to design a β-solidifying TiAl based alloy which exhibits an adjustable volume fraction of β-phase. In the as-cast state the selected alloy Ti-43Al-4Nb-1Mo-0.1B shows a microstructure consisting of equiaxed lamellar (γ +α_2)-colonies with a colony diameter of about 100 μm. The β/B2-phase is mainly located along colony boundaries. Texture analysis using neutron diffraction has shown no occurrence of a casting texture. A subsequent hot extrusion process leads to a pronounced refinement of the microstructure. At temperatures where hot-deformation processes, such as forging and rolling are conducted, the amount of β/B2-phase is

considerably high in order to facilitate plastic deformation. However, the fraction of the β/B2-phase exhibits a minimum around the α-transus temperature which is reflected in a maximum of the flow stress. At service temperature (T < 800°C), however, the volume fraction of the β/B2-phase is designed to be small in order not to deteriorate mechanical properties, e.g. creep strength. The evolution of the β/B2-phase with temperature was investigated in-situ by means of high-energy XRD as well as conventional ex-situ characterization methods. In principle, the results obtained experimentally confirm the temperature dependence of the β/B2-phase as predicted by thermodynamic calculations, although the question concerning the existence of a single α phase field could not be answered. Due to a high volume fraction of β/B2-phase at elevated temperatures the alloy can be forged under near conventional conditions. Alloy Ti-43Al-4Nb-1Mo-0.1B shows a large forging window with regard to billet temperature, die temperature, and die speed, providing the basis for a robust industrial forging process.

Acknowledgement

The authors thank Prof. Brokmeier, GKSS Research Centre, Geesthacht, Germany, for texture measurements and LaReine A. Yeoh, ANSTO, Australia, for participation in the synchrotron experiments. A part of this study has been supported by the Styrian Materials Cluster, Austria. In addition, the authors are grateful for the beam-time and overall support delivered at ESRF, Grenoble, France. We also acknowledge financial support from the Access to Major Research Facilities Program which is a component of the International Science Linkages Program from the Australian Government. In particular, H.C. thanks Arno Bartels for many stimulating discussions and real friendship over the last 17 years.

Literature

1. Gamma titanium aluminides 2003, Kim Y-W, Clemens H, Rosenberger AH, editors. Warrendale, USA: TMS; 2003.
2. Appel F, Oehring M. In: Leyens C, Peters M, editors. Titanium and titanium alloys. Weinheim, Germany: WILEY- VCH; 2003. p. 89.
3. Kestler H, Clemens H. In: Leyens C, Peters M, editors. Titanium and titanium alloys. Weinheim, Germany: WILEY- VCH; 2003. p. 351.
4. Appel F, Oehring M, Wagner R. Intermetallics 2000;8:1283.
5. Appel F, Brossmann U, Christoph U, Eggert S, Janschek P, Lorenz U, Müllauer J, Oehring M, Paul JDH. Adv Eng. Mater. 2000;11:699.
6. Leyens C. In: Leyens C, Peters M, editors. Titanium and titanium alloys. Weinheim, Germany: WILEY- VCH; 2003. p. 187.
7. Küstner V, Oehring M, Chatterjee A, Güther V, Brokmeier H.-G, Clemens H. In: Kim Y-W, Clemens H, Rosenberger AH, editors. Gamma titanium aluminides 2003. Warrendale, USA: TMS; 2003. p. 89.
8. Küstner V. PhD thesis, Christian-Albrechts-Universität zu Kiel. Kiel, Germany: 2003.
9. Imayev RM, Imayev VM, Oehring M, Appel F. Intermetallics 2007;15:451.
10. Tetsui T, Shindo K, Kobayashi S, Takeyama M. Scripta Mater 2002;47:399.
11. Tetsui T, Shindo K, Kobayashi S, Takeyama M. Intermetallics 2003;11:299.
12. Tetsui T, Shindo K, Kaji S, Kobayashi S, Takeyama M. Intermetallics 2005;13:971.
13. Appel F, Oehring M, Paul JDH. Adv Eng Mater 2006;8:371.
14. Cheng TT, Loretto MH. Acta Mater 1998;46:4801.

15. Chladil HF, Clemens H, Zickler GA, Takeyama M, Kozeschnik E, Bartels A, Bulaps T, Gerling R, Kremmer S, Yeoh L, Liss KD. Int. J. Mat. Res. (formerly Z. Metallkunde) 2007;98:1131.

16. Chladil HF. PhD thesis, Montanuniverstät. Leoben, Austria: 2007.

17. Chladil HF, Clemens H, Otto A, Güther V, Kremmer S, Bartels A, Gerling R. Berg- und Hüttenmännische Monatshefte (BHM) 2006;151:356.

18. Kremmer S, Chladil HF, Clemens H, Otto A, Güther V. In: Niinomi M, Akiyama S, Hagiwari M, Ikeda M, Maruyama K, editors. Ti-2007 science and technology. Tokyo, Japan: The Japan Institute of Technology; 2008. p. 989.

19. Takeyama M, Kobayashi S. Intermetallics 2005;13:993.

20. Appel F, Paul JDH, Oehring M, Fröbl U, Lorenz U. Metall. Mater. Trans. A 2003;34:2149.

21. Saunders N. In: Kim Y-W, Dimiduk DM, Loretto MH, editors. Gamma titanium aluminides 1999. Warrendale, USA: TMS; 1999. p. 183.

22. Chladil H, Clemens H, Leitner H, Bartels A, Gerling R, Schimansky FP, Kremmer S. Intermetallics 2006;14:1194.

23. Kainuma R, Fujita Y, Mitsui H, Ohnuma I, Ishida K. Intermetallics 2000;8:855.

24. Zhang Z, Leonard KJ, Dimiduk DM, Vasudevan VK. In: Hemker KJ, Dimiduk DM, Clemens H, Darolia R, Inui H, Larsen JM, Sikka VK, Thomas M, Whittenberger JD, editors. Structural intermetallics 2001. Warrendale, USA: TMS; 2001. p. 515.

25. Kim Y-W, Dimiduk DM. In: Hemker KJ, Dimiduk DM, Clemens H, Darolia R, Inui H, Larsen JM, Sikka VK, Thomas M, Whittenberger JD, editors. Structural intermetallics 2001. Warrendale, USA: TMS; 2001. p. 625.

26. Güther V, Chatterjee A, Kettner H. In: Kim Y-W, Clemens H, Rosenberger AH, editors. Gamma titanium aluminides 2003. Warrendale, USA: TMS; 2003. p. 241.

27. Dahms M, Bunge HJ. J Appl Cryst 1989;22:439.

28. Hammersley AP, Svensson SO, Hanfland M, Fitch AN, Häusermann D. High Press Res 1996;14:235.

29. Yamaguchi M, Inui H, Ito K. Acta Mater 2000;48:307.

30. Bartels A, Kestler H, Clemens H. Mat Sci Eng A 2002;329-331C:152.

31. Liss KD, Bartels A, Clemens H, Bystrzanowski S, Stark A, Buslaps T, Schimansky FP, Gerling R, Scheu C, Schreyer A. Acta Mater 2006;54:3721.

32. Walgram W. Diploma thesis, Montanuniverstät. Leoben, Austria: 2008.

33. Porter DA, Easterling KE. Transformations in metals and alloys. Cheltenham, UK: Nelson Thornes Ltd.; 2001. p. 139.

34. Appel F, Kestler H, Clemens H. In: Westbrook JH, Fleischer RL, editors. Intermetallic compounds – principles and practice, volume 3, progress. Chicester, UK: John Wiley Publishers; 2002. p. 617.

Figure Captions

Figure 1: Calculated phase fractions as a function of temperature for the investigated alloy Ti-43Al-4Nb-1Mo-0.1B including 450 mass-ppm oxygen. Note the temperature dependence of the β-phase. The phase fraction of β-phase decreases from the eutectoid temperature (here at ~ 1115°C) towards the α-transus temperature (T_α ~ 1265°C), exhibits a minimum at T_α and increases again for temperatures above T_α.

Figure 2: (a) Microstructure of alloy Ti-43Al-4Nb-1Mo-0.1B in as-cast condition. Inset: detail in larger magnification. (b) Microstructure of the same alloy after hot-extrusion below the α-transus temperature. The extrusion direction is vertical; extrusion ratio: ~ 7:1. Arrows: borides aligned in extrusion direction. SEM images taken in back-scattered electron (BSE) mode, i.e. γ-TiAl appears grey to dark, α_2-Ti_3Al light grey and β exhibits the brightest contrast.

Figure 3: Recalculated 110 - pole figure of the γ-TiAl phase in alloy Ti-43Al-4Nb-1Mo-0.1B after casting and solidification. A maximum pole density of 1.8 multiple random distribution (MRD) suggests no statistically significant texture. Inset: 110 - pole figure of an arc-melted Ti-48Al button (2.64 MRD). A well developed casting texture is present (see text and ref. [7]).

Figure 4: A series of HE-XRD patterns (azimuthally averaged scattering intensity versus |scattering vector| q) during continuous heating of the alloy Ti-43Al-4Nb-1Mo-0.1B at (a)

21°C, (b) 1179°C, (c) 1259°C and (d) 1320°C. The diffraction peaks are indexed according to the present phases: (a) γ, α_2 and B2, (b) γ, α and B2, (c) γ, α and B2, (d) α and β/B2.

Figure 5: Microstructure of a Ti-43Al-4Nb-1Mo-0.1B sample after annealing within the single α-phase region at 1270°C for 3 hrs. The starting microstructure is shown in Figure 2b. During annealing the α-grains have grown to an average diameter of about 200 μm. The remaining β-phase (bright contrast) is partly situated along former α-grain boundaries and triple points. During subsequent air cooling the α-grains transformed to lamellar (α_2 + γ)-colonies. SEM image taken in BSE mode.

Figure 6: Dependence of the flow stress of hot-extruded alloy Ti-43.8Al-4Nb-1Mo-0.1B on temperature and strain rate (here 0.05 and 0.5 s^{-1}). Because of confidentiality reasons the numerical values of the flow stresses have been omitted. The temperature (~T_α) where the maximum of the flow stress occurs corresponds with that temperature where CHAPHAD predicts the minimum fraction of β-phase (Figure 1).

Figure 7: (a) Pancake of Ti-43Al-4Nb-1Mo-0.1B. The billet was forged to an overall strain of 1.3. (b) Microstructure of the forged pancake. The microstructure consists of lamellar (α_2 + γ)-colonies with β-phase (bright contrast) situated on colony boundaries and triple points. SEM image taken in BSE mode. (c) Ground blade pre-form manufactured by upsetting both sides of a cylindrical bar and subsequent side pressing to the final shape.

Figures

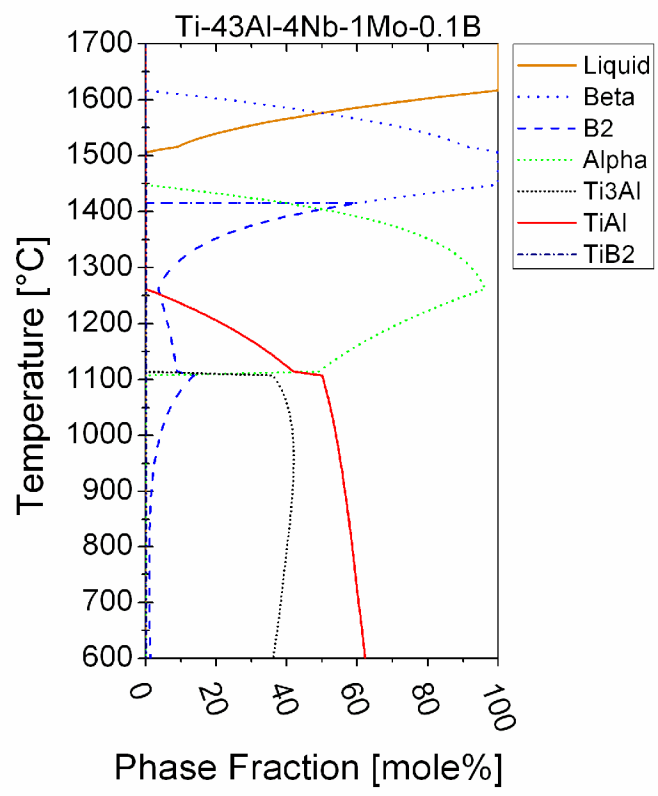

Figure 1

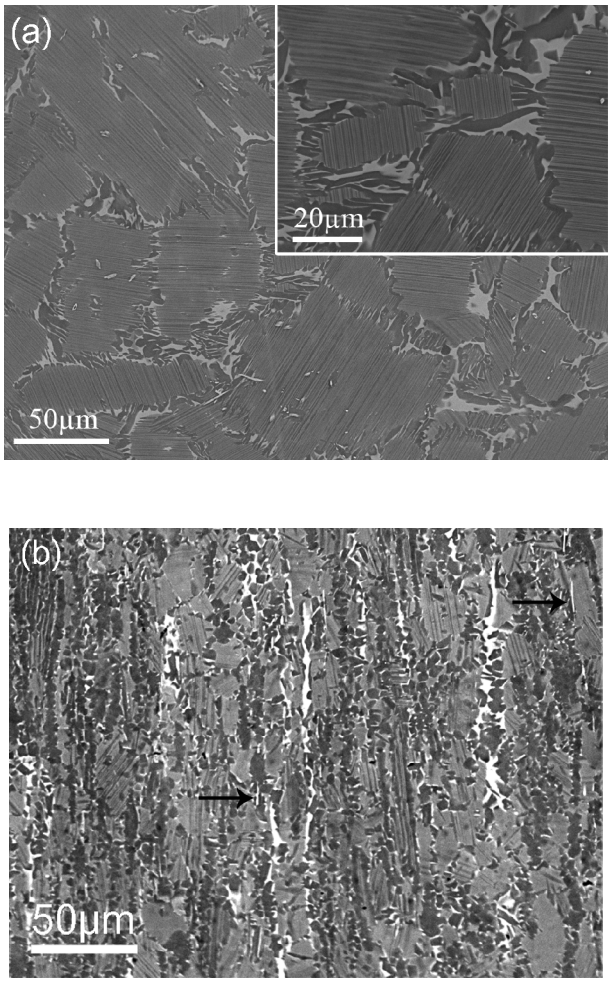

Figure 2

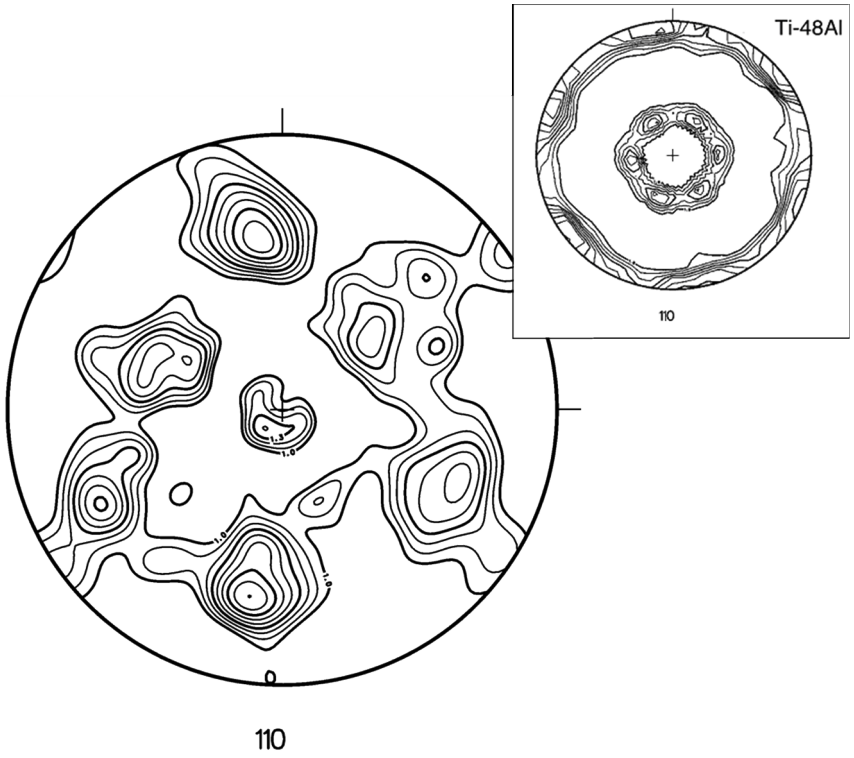

Figure 3

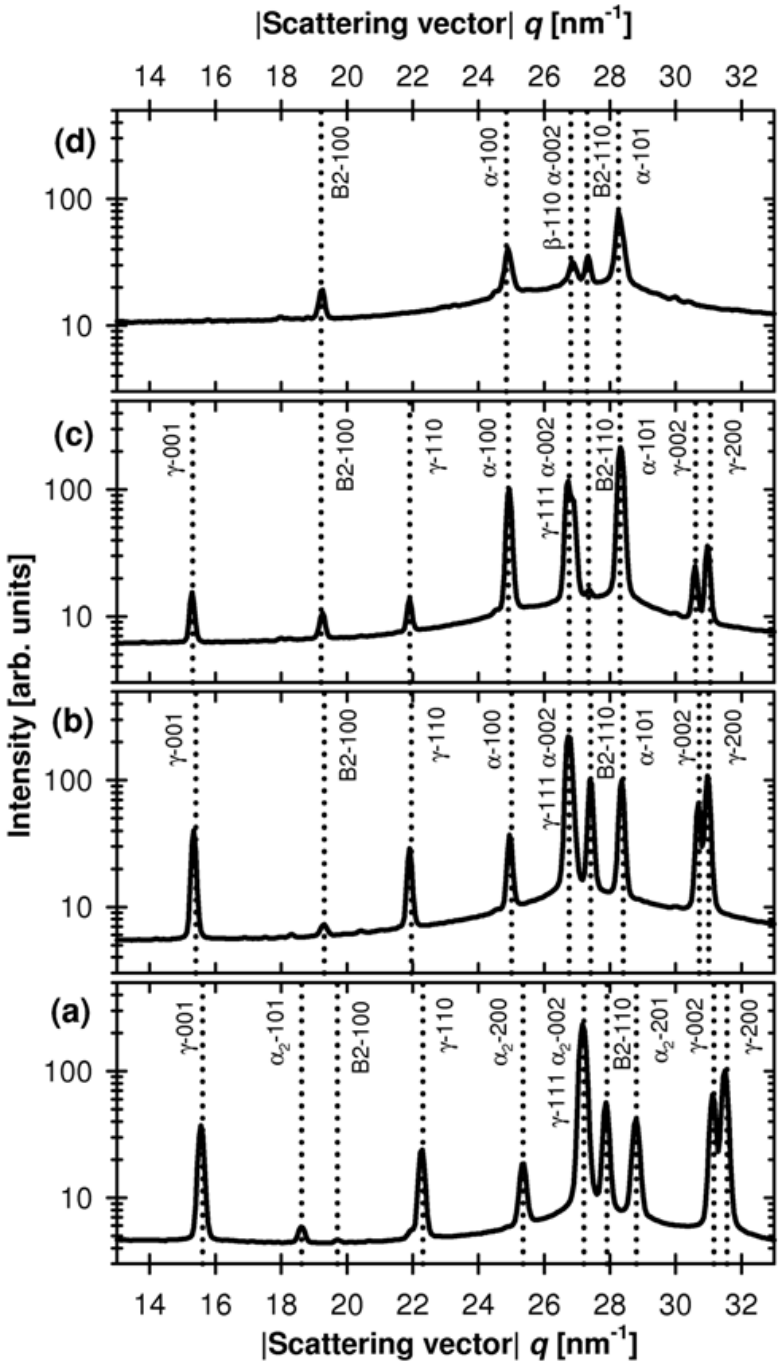
|Scattering vector| q [nm-1]
14 16 18 20 22 24 26 28 30 32
(d)
B2-100
α-100
β-110 α-002
B2-110
α-101
(c)
γ-001
B2-100
γ-110
α-100
γ-111 α-002
B2-110
α-101
γ-002
γ-200
(b)
γ-001
B2-100
γ-110
α-100
γ-111 α-002
B2-110
α-101
γ-002
γ-200
(a)
γ-001
α2-101
B2-100
γ-110
α2-200
γ-111 α2-002
B2-110
α2-201
γ-002
γ-200
100
10
Intensity [arb. units]
|Scattering vector| q [nm-1]

Figure 4

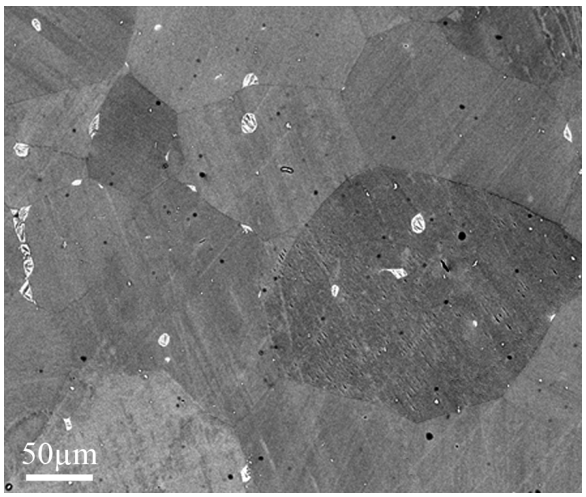

Figure 5

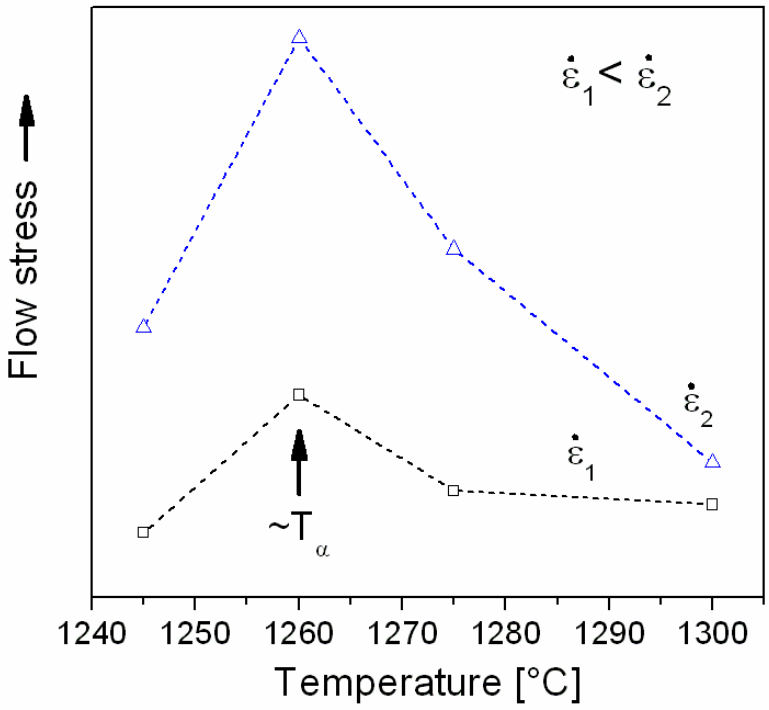
Flow stress
$\dot{\varepsilon}_1 < \dot{\varepsilon}_2$
$\dot{\varepsilon}_2$
$\dot{\varepsilon}_1$
$\sim T_\alpha$
1240
1250
1260
1270
1280
1290
1300
Temperature [°C]

Figure 6

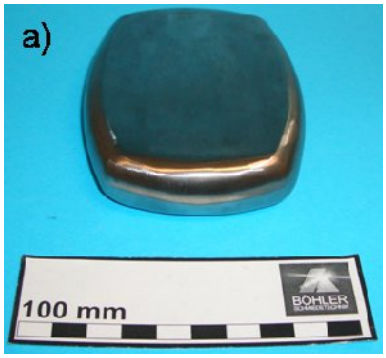

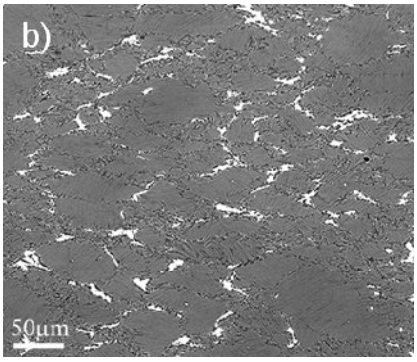

Figure 7 a) – c)

Table

Table 1: Transformation temperatures and corresponding phase fields of alloy Ti-43Al-4Nb-1Mo-0.1B as determined by in-situ high-energy X-ray diffraction. The determined temperatures fit well to the results obtained from DSC measurements and the evaluation of static heat-treatments [17,32].

phase field	α, β/B2
α-transus temperature	1285°C±5°C*
phase field	α, B2, γ
eutectoid temperature	1165°C±5°C
phase field	α_2, B2, γ

*The discrepancy between the α transus temperature determined by HE-XRD and DSC measurements is most likely due to the finite heating rate of the in-situ XRD experiment. This divergence is not observed at the eutectoid temperature, because the ordering reaction from α_2 to α is rather fast compared to the α transus reaction.